Review Article

Ali N. Hamoodi*, Safwan A. Hamoodi and Rasha A. Mohammed

Partial discharge calibrator of a cavity inside high-voltage insulator

https://doi.org/10.1515/eng-2022-0048
received February 27, 2022; accepted May 24, 2022

Abstract: This article displayed the method of partial discharge (PD) measurement in high-voltage insulator and calibrating the effective element (capacitor) to enhance the PD signal. The cavity shapes were plate–plate, cylindrical and spherical inside the solid insulator. The proposed system enables from detecting the reverse and main discharge, respectively, through the rise and tail time of the pulses. PD that took place was bounded with internal cavities. Proteus simulator and Matlab simulation models were used to measure and display the PD signal. The results showed PD-calibrated waveforms and the voltage values across the cavity (V_c). Finally, this work concluded that the spherical cavity shape gave a higher value of the calibrated capacitor and lower voltage across the cavity (V_c) for both models.

Keywords: partial discharge, cavity shapes, Proteus simulator, Matlab/Simulink, PD calibrator

1 Introduction

Partial discharge (PD) measurement produces a salutary tool to acquire information about discharging taints in high-voltage (HV) insulators. PD occurs in the cavity inside the insulators. Thus, PD measurements in insulators are deemed a salutary instrument to diagnose the insulation conditions for on-site and laboratory applications.

PD taking place in a void inside insulators, and internal PD or cavity PD have made much attention majorly for two reasons: (1) PD demeanor is closely opposite to the characteristics of dielectric and the second, excited molecules, the ion bombardment, and localize temperature rise generated by PDs will deteriorate due to performance of insulation. PD happens due to the defect on the insulation surface or inside it when the electric field applied to overcome the dielectric strength of the insulation medium.

The purpose of PD measurement is to detect what the problem may have occurred in HV insulators before failure events. Laboratory tests showed that most HV insulators gradually deteriorate over many years. By routinely measuring the PD activity every 6 months, insulation deterioration can be rapidly identified and suitable maintenance has to be performed [1–4].

Many studies have been carried out to attain the impact of each parameter of the environment on the PD properties of HV insulators. This article is composed as follows: Section 2 presents the literature review. Section 3 presents the layout and circuit diagram. Section 4 presents the calibration of the PD measuring circuit. Section 5 presents verification of the PD measuring system. Section 6 presents the simulated mode for detection of PD by Proteus. Section 7 presents results and discussion. Section 8 concludes this article. Section 9 presents the future scope.

2 Literature review

Gunawardana et al. worked on PD detection in HV equipment (solid insulators). They used Matlab/Simulink package for PD detection simulation. A cylindrical void inside an epoxy resin insulator was adopted in the developed model. They concluded that the results obtained by Simulink were highly similar to the results obtained by an actual published PD measuring system [5].

Arief et al. studied the deliberating PD meter. They took a voltage pulse as a source with coupling capacitors. They worked on the calibrator to imitate the real test sample to be more accurately than an electronic. Then, they concluded the ability and possibility to use this kind of calibrator for mutual relative comparison [6].

* **Corresponding author: Ali N. Hamoodi,** Department of Electrical Power Techniques Engineering, Northern Technical University, Technical College of Engineering, Mosul, Iraq, e-mail: ali_n_hamoodi74@ntu.edu.iq, tei: +964-770-876-2558
Safwan A. Hamoodi: Department of Electrical Power Techniques Engineering, Northern Technical University, Technical College of Engineering, Mosul, Iraq, e-mail: safwan79azb@ntu.edu.iq
Rasha A. Mohammed: Department of Electrical Power Techniques Engineering, Northern Technical University, Technical College of Engineering, Mosul, Iraq, e-mail: Rashana8479@ntu.edu.iq

3 Methodology

To calibrate the measurement system, a calibration pulse has been injected into the system of the PD measurement. The shape of the calibration pulse must be identical to the standard pulse shape. The internal cavities inside the solid dielectric are the mean cause of the PD. The charge of PD has been injected between the terminals of the test sample and measured as a voltage and current pulses by using the general PD measuring circuit. The contribution of this work was to enhance the PD pulse shape arriving at the criterion shape [7–9].

3.1 Layout and circuit diagram

A PD measurement circuit diagram is illustrated in Figure 1. To determine the primal amount of PD pulse, a simple-minded equivalent capacitor circuit of the cavity inside the insulator is utilized by Matlab/Simulation. The equivalent circuit of different cavity shapes (plate–plate, cylindrical, and spherical) was considered in this work to find the PD pulses. Different types of void capacitors were calculated as their equations and substituted them in the modeling circuit [10–12].

3.2 PD calibrator circuit

The amount appraisal of the apparent charge (q_a) moved from the PD resource to the test sample terminal in the Gemant and Philipp off method, often indicated as a, b and c model because of the characteristics of capacitors. Because of the series connection of C_c and C_b, where the circumstance ($C_b/C_c \ll 1$) is semper gratified, the (q_a) discoverable on the test sample terminals is expressed as follows [13–16]:

$$q_a = q_c \times \frac{C_b}{C_c}, \tag{1}$$

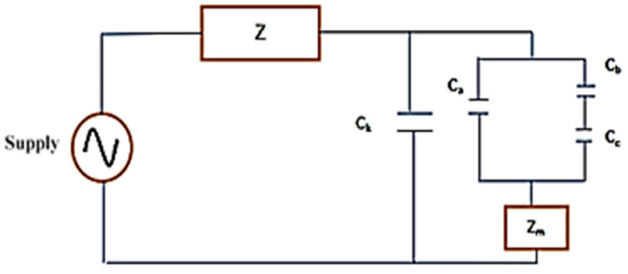

Figure 1: Circuit diagram of PD measurement.

where
C_a is the apparent capacitor,
C_b is the rest of the insulator capacitor,
C_c is the cavity capacitor,
q_a is the apparent charge and
q_c is the pulse charge.

The fathomable q_a is merely a small portion of the real pulse charge q_c generated in the PD resource. Thus, the PD tightness of HV device cannot be used to assess solitary because the ratio C_b/C_c is not savvied. Thus, the norms for PD description were found in the past, which were dictated on practical experiments earned from inclusive PD studies on-site and in laboratory.

The charge transfer form PD resource and HV terminals device. The adaptation of the calibrator according to these procedures the q_a for a PD pulse is appointed in IEC60270, if the q_a injected during a sorely short time across the test example terminals would yive similar readings on the measurement tool. PD calibrator commonly represents the pulse generator that is connected serially with calibrator capacitors. The transient voltages on the PD imperfection pulse generator edify equal potential strides of discerned magnitudes U_o. When the calibrator capacitor C_o value is lesser than the presumptive test sample capacitor C_a value, the injected charge inside the test sample is given by [17–23]:

$$q_o = C_o \times U_o = C_a \times U_1, \tag{2}$$

and

$$q_a = C_a \times U_2. \tag{3}$$

By substituting equation (2) into equation (3), we obtain

$$q_a = q_o \times (U_2/U_1). \tag{4}$$

The transient voltage U_2 and U_1, which appear across C_a, helps to obtain the scale factor results from the two readings of R_i and R_o, and equation (4) can be rewritten as follows:

$$q_a = q_o \times (R_i/R_o). \tag{5}$$

PD calibrator circuit can be drawn as a pulse generator connected in serially with calibrating capacitor and the produced pulses represent the injected charge q_o as shown in Figure 2 [24,25].

$$q_o = U_o \times C_o, \tag{6}$$

where
U_o is the inp. step voltage,
C_o is the calibrator generator capacitor,
U_m is the out. voltage across R_m,
q_o is the injected charge,
U_1, U_2 are transient voltages and
R_i/R_o is the scale factor.

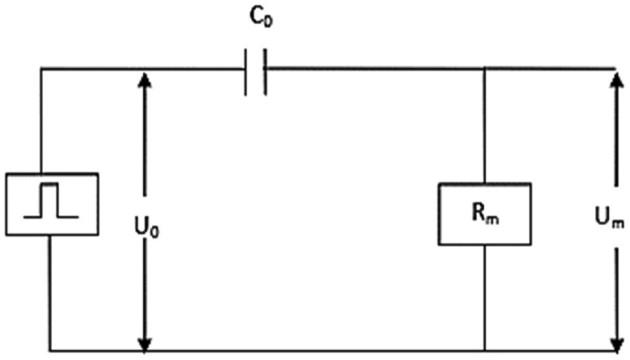

Figure 2: PD pulse generator.

3.3 Cavity properties

The cavity types, shapes and equations are listed in Table 1.

Plate-to-plate capacitor has distance between two plates (1 mm) with different areas, and spherical capacitor has (a) inner and (b) outer radii. Length (L), inner radii (a) and outer radii (b) of a cylindrical capacitor were taken from depended HV cavities [26,27]. The parameters readings are listed in Table 2.

3.4 Calibrator circuit model results

PD calibrator circuit consists of Arduino kit, push bottoms, capacitors and measurement resistance as shown in Figure 3. Arduino pulse generator was connected serially with a parallel set of switching capacitors. The changeable charge level was obtained by switching the various capacitors. X-axes and Y-axes represent the time in seconds and PD calibrator voltage signal, respectively.

Table 1: Cavity shape, equation and value inside HV insulators

Capacitor type	Figure	Equation
Plate–plate capacitor with plate area A and the distance between two plates d	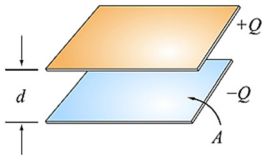	$C = \varepsilon_0 \frac{A}{d}$
Cylindrical capacitor with length L, inner radius a and outer radius b	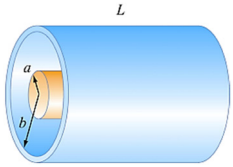	$C = \frac{2\pi\,\varepsilon_0 L}{\ln(b/a)}$
Spherical capacitor with inner radius a and outer radius b	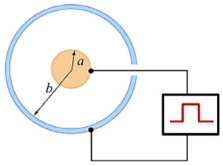	$C = 4\pi\varepsilon_0 \frac{a\,b}{(b-a)}$

Table 2: Switching capacitors used in Proteus simulation

Sl. No.	Parameters	Values (nF)		
		Plate–plate	Cylindrical	Spherical
1	Capacitor 1	20	100	180
2	Capacitor 2	40	120	200
3	Capacitor 3	60	140	220
4	Capacitor 4	80	160	240
5	Resistor	100	**100**	100

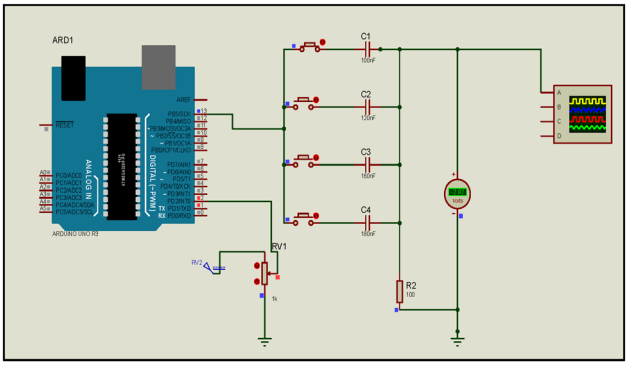

Figure 3: PD calibrator circuit-based Arduino.

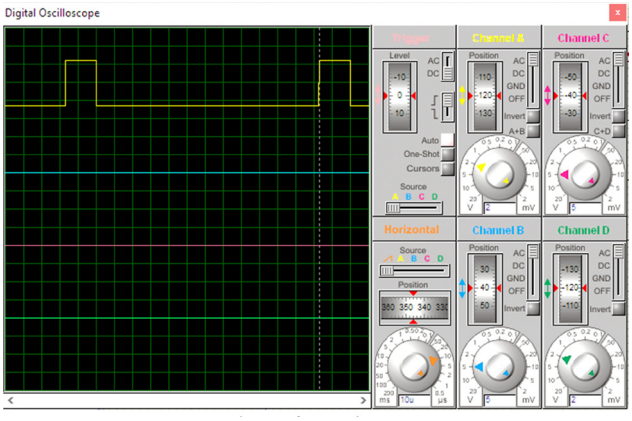

Figure 4: Pulse signal on Proteus.

Table 3: Pulse parameters

Sl. No.	Parameters	Values
1	Initial value V_1	0 V
2	Pulse value V_2	5 V
3	Pulse fall time t_f	10–9 s
4	Pulse delay time t_d	0 s
5	Pulse rise time t_r	10^{-9} s
6	Pulse width pw	0.175×10^{-4} s
7	Pulse period per	1.4×10^{-4} s

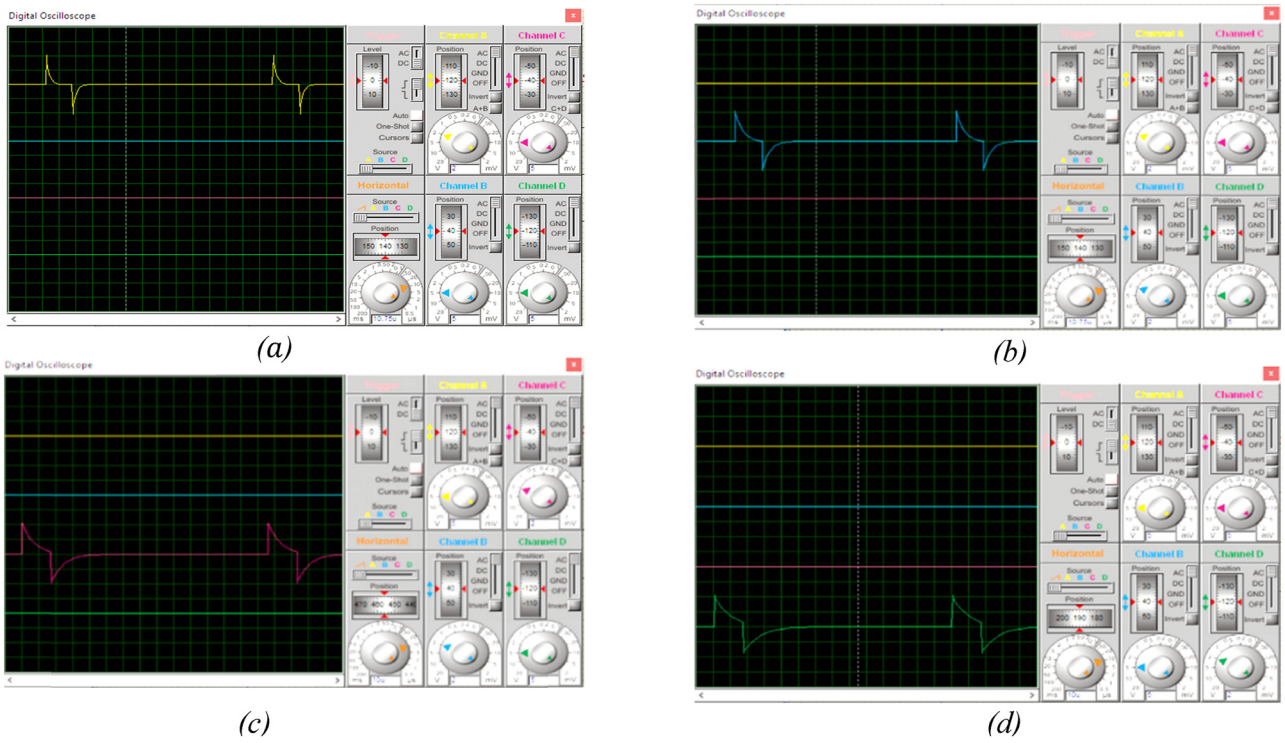

Figure 5: PD signals due to the effect of the calibrating capacitors (plate–plate). (a) PD signal with respect to C_1. (b) PD signal with respect to C_2. (c) PD signal with respect to C_3. (d) PD signal with respect to C_4.

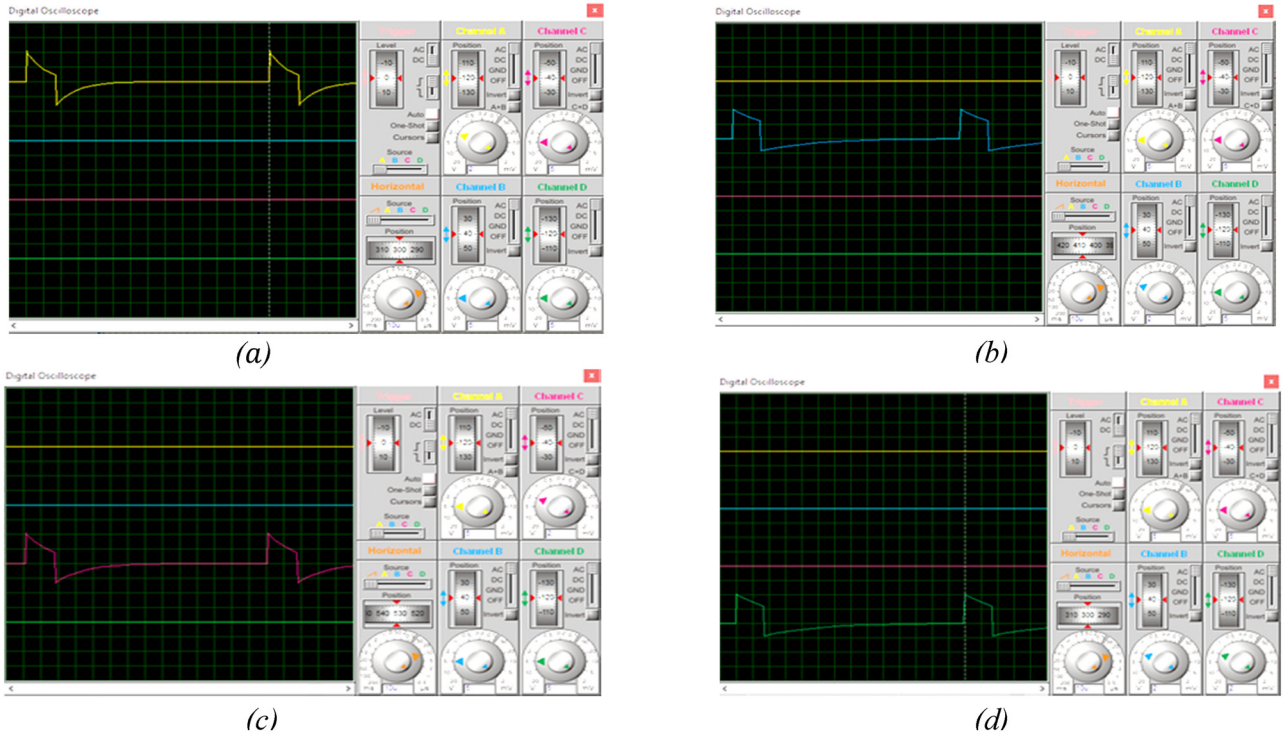

Figure 6: PD signals due to the effect of the calibrating capacitors (cylindrical). (a) PD signal with respect to C_1. (b) PD signal with respect to C_2. (c) PD signal with respect to C_3. (d) PD signal with respect to C_4.

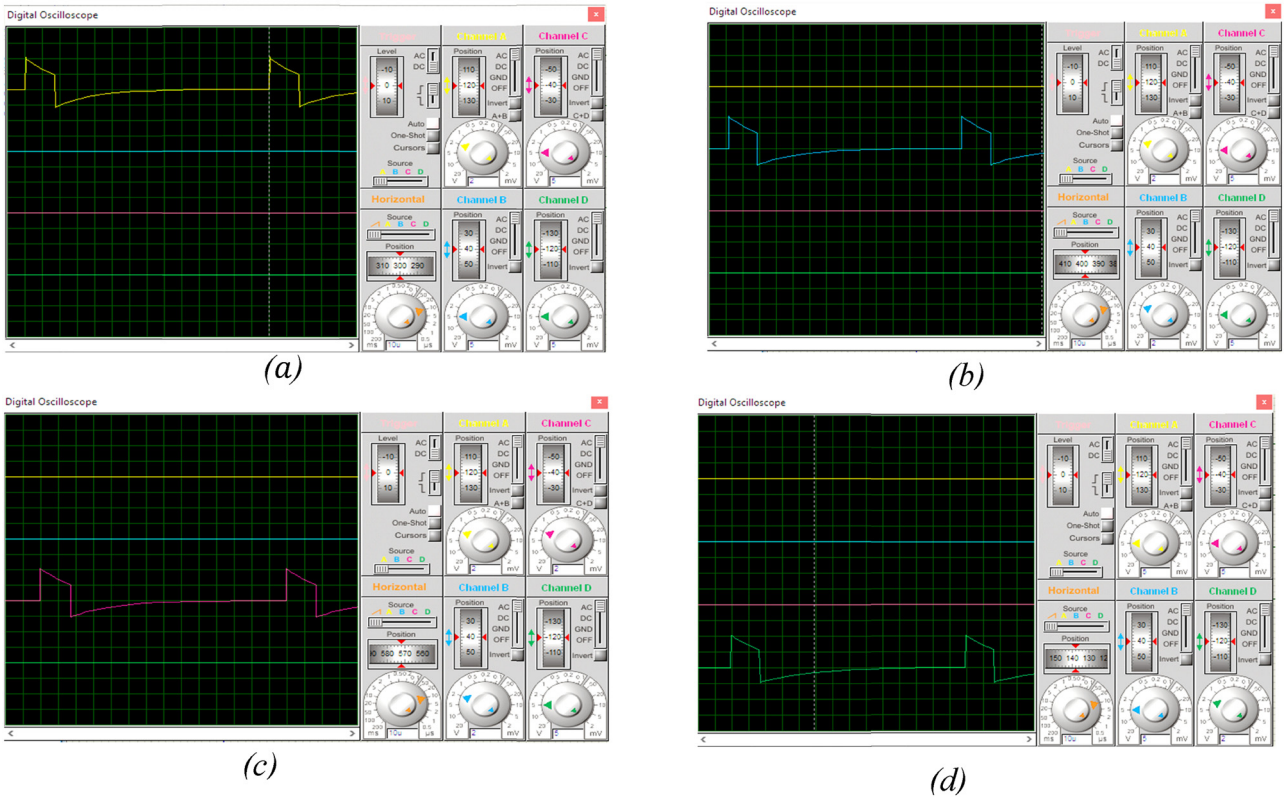

Figure 7: PD signals due to the effect of the calibrating capacitors (spherical). (a) PD signal with respect to C_1. (b) PD signal with respect to C_2. (c) PD signal with respect to C_3. (d) PD signal with respect to C_4.

Arduino pulse signal was produced by the uploaded code and ran on the Proteus simulator as shown in Figure 4.

The pulse shape parameters that were as shown in Figure 4 are listed in Table 3.

3.5 Plate-to-plate capacitor type

PD signals across the measurement resistor (R_m), which are produced due to the calibrating capacitors C_1, C_2, C_3 and C_4, are depicted in Figure 5.

3.6 Cylindrical capacitor type

PD signals across the measurement resistor (R_m), which are produced due to the calibrating capacitors (C_1, C_2, C_3 and C_4), are depicted in Figure 6.

3.7 Spherical capacitor type

PD signals across the measurement resistor (R_m), which produced due to the calibrating capacitors (C_1, C_2, C_3 and C_4), are depicted in Figure 7.

3.8 PD measuring circuit results

Figure 8 represents the PD measurement signal, and it consists of HV supply, impedance (Z) capacitor (C_k), apparent capacitor (C_a), remaining series capacitor (C_b), void capacitor (C_c) and RLC measuring circuit. When a HV supply was applied to this circuit, discharge occurred. The measuring circuit (RLC) was connected in series, which forded the detecting circuit to receive this pulse

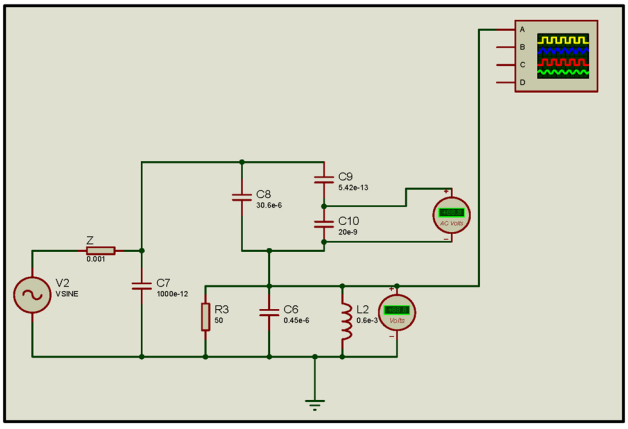

Figure 8: PD measurement circuit.

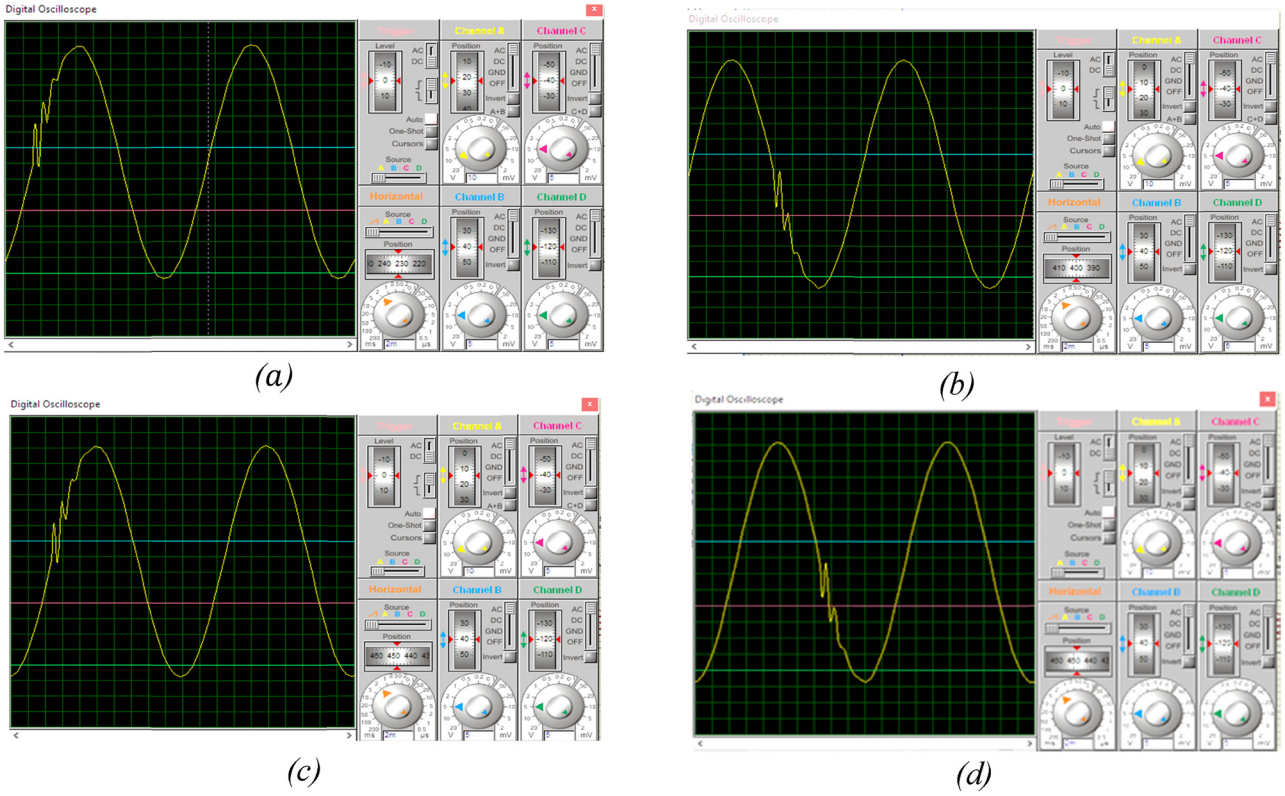

Figure 9: PD location. (a) PD hit due to C_1. (b) PD hit due to C_2. (c) PD hit due to C_3. (d) PD hit due to C_4.

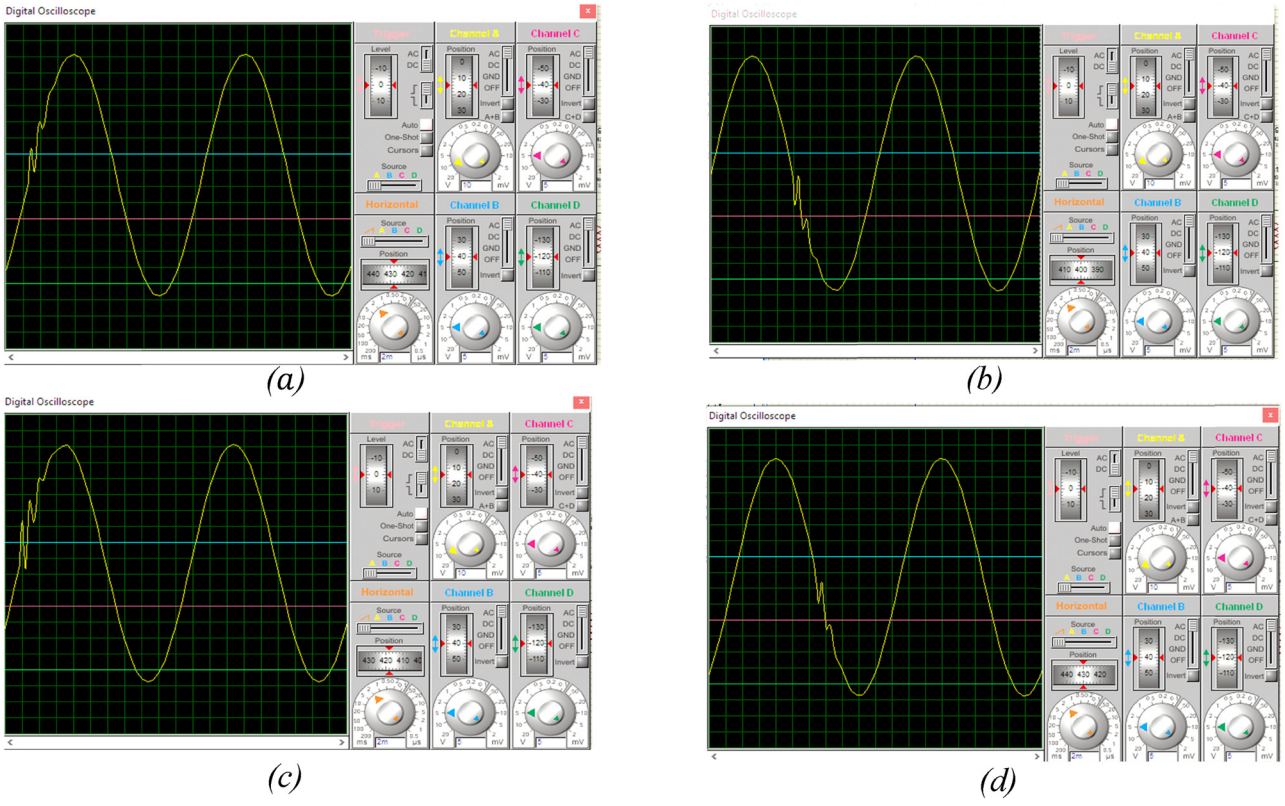

Figure 10: PD location. (a) PD hit due to C_1. (b) PD hit due to C_2. (c) PD hit due to C_3. (d) PD hit due to C_4.

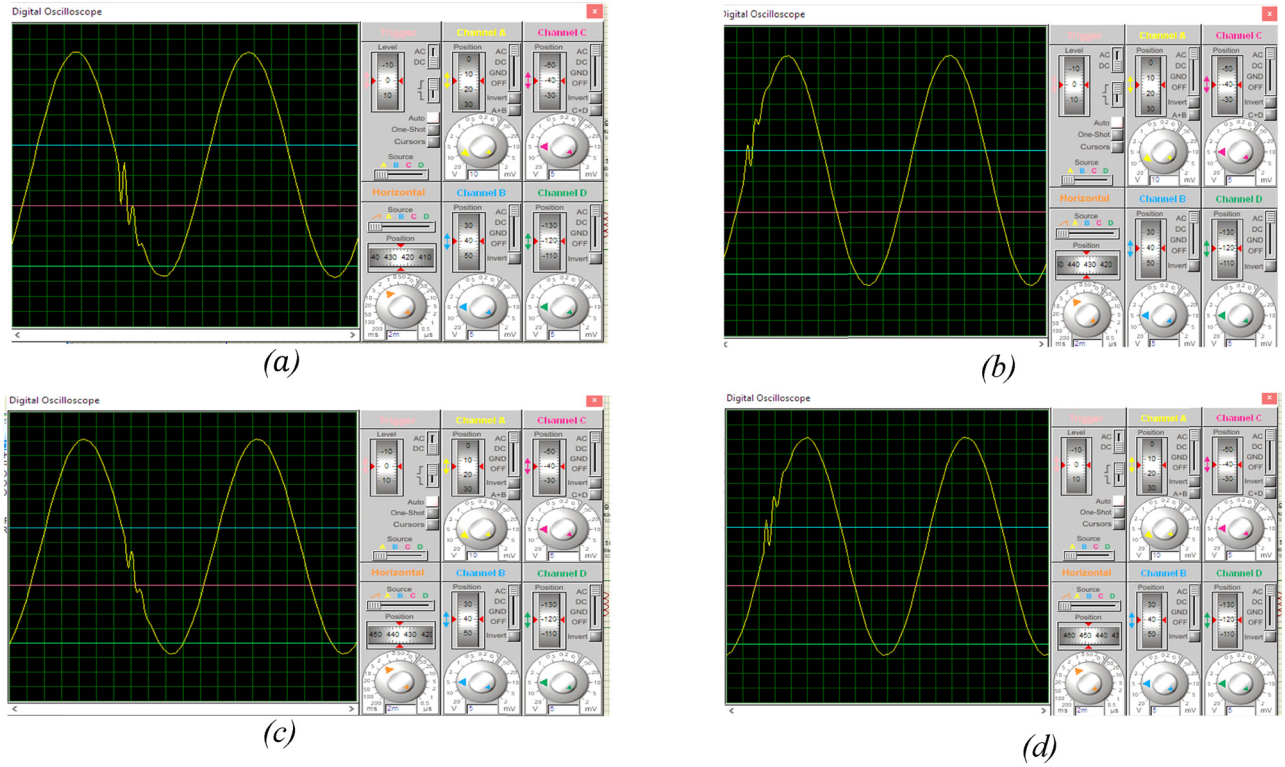

Figure 11: PD location. (a) PD hit due to C_1. (b) PD hit due to C_2. (c) PD hit due to C_3. (d) PD hit due to C_4.

from the test sample. The sinusoidal waveforms in Section 8 were created from the PD measuring circuit as shown in Figure 1, where a sine wave voltage source has been applied. The *X*-axes and *Y*-axes represent the time in seconds and PD hit voltage signal, respectively.

3.9 Plate-to-plate capacitor type

Figures (9–11) represent the location and voltage value of PD due to the effect of C_1, C_2, C_3 and C_4.

The location of PD due to plate-to-plate cavity with different sizes is shown in Figure 9.

3.10 Cylindrical capacitor type

The location of PD due to the cylindrical cavity with different sizes is depicted in Figure 10.

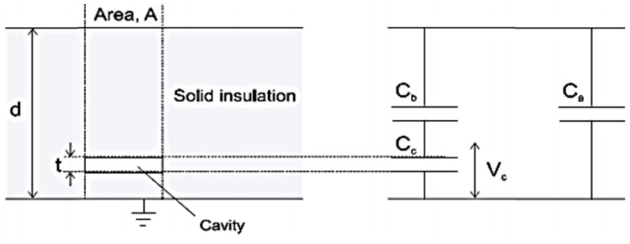

Figure 12: Capacitor model of cavity in insulation.

Table 4: Cavity voltage for three types of capacitors

C (nF)	V_c (V)
20	0.77
40	0.39
60	0.26
80	0.19
100	0.15
120	0.13
140	0.11
160	0.09
180	0.08
200	0.07
220	0.06

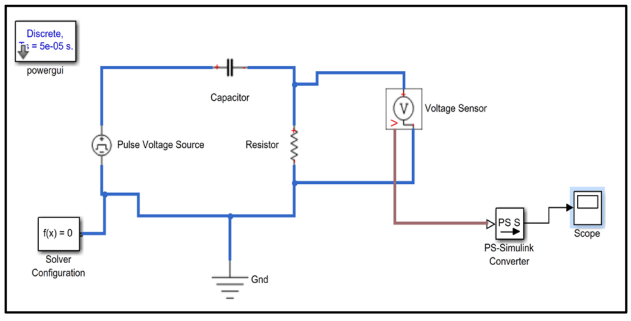

Figure 13: Matlab modeling of the PD-calibrated circuit.

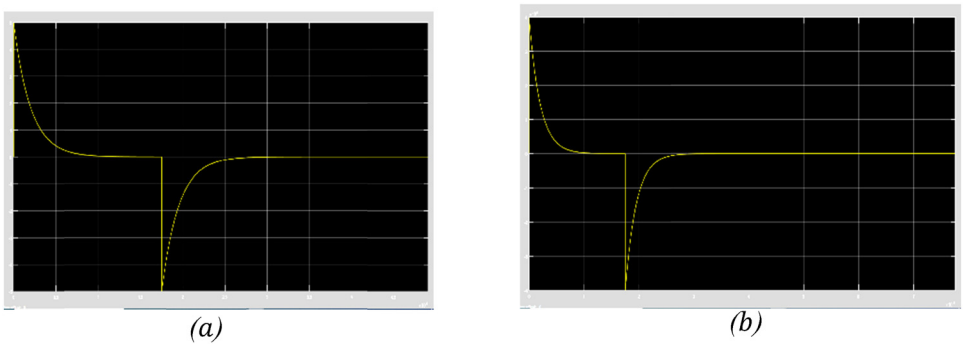

Figure 14: PD calibrated signals from Matlab/Simulink. (a) Pulse voltage source (40 kV). (b) Pulse applied (5 V).

3.11 Spherical capacitor type:

The location of PD due to the cylindrical cavity with different sizes is illustrated in Figure 11.

Solid insulation with voids or cavities leading to this model is depicted in Figure 12.

The capacitor C_a is computed as follows:

$$C_a = \frac{\varepsilon_o \varepsilon_r A}{d}, \tag{7}$$

where ε_o is the free space permittivity, ε_r is the solid insulating permittivity,

A is the area between electrodes, and d is the insulation thickness.

Hence, the capacitor of the cavity is given by this equation:

$$C_c = \frac{\varepsilon_o A}{t}, \tag{8}$$

where t is the cavity voids thickness.

The capacitor of the insulation in series with C_c is given in the following equation:

$$C_b = \frac{\varepsilon_o \varepsilon_r A}{d}. \tag{9}$$

Therefore, the voltage across the cavity can be expressed by the following equation:

$$V_c = \frac{C_b}{C_c + C_b} \times Va. \tag{10}$$

From the Proteus simulator, the voltage value across each capacitor for three types (plate–plate, cylindrical, and spherical) are listed in Table 4.

3.12 Matlab modeling

PD calibrator circuit based Matlab/Simulink representation is given in Figure 13. Pulse voltage source with HV value 40 kV the output signal that appeared from this source value was compared with the output signal that obtained from the scaled value 5 V (scaling factor 1/8).

Figure 14 shows the PD-calibrated signal for both sources (40 kV and 5 V), which appeared similarly in the applied both sources.

4 Conclusion

The pulse generated from Arduino Kit has parameters closed to ideal pulse for the same thickness of cavity, and the capacitor of this cavity was different from one to another one due to the different shapes of the cavity. Higher capacitor values of the cavity gave lower voltage across it which in turn gave lower PD inside it. Spherical cavity reduced from PD severity.

5 Future scope

The improved method by the equivalent circuit of PD calibrator is needed that included arbitrary waveform generator, connecting lead and control measurement.

Acknowledgements: We would like thank our affiliation of Northern Technical University Technical College of Engineering, Mosul-Iraq.

Conflict of interest: The authors state no conflict of interest.

References

[1] Chen HAG, Lewin PL. Measurement and modelling of partial discharge behaviour in a spherical cavity within a solid

dielectric material as a function of applied voltage amplitude, 978-1-4244-8286-3/10/$26.00 ©IEEE; 2010.
[2] Paoletti GJ, Golubev A. Partial discharge theory and applications to electrical systems. Presented at the 1999 IEEE IAS Pulp and Paper Industry Conference in Seattle. WA: © IEEE 1999-Personal use of this material is permitted.
[3] Hameed FI, Hamoodi AN, Mohammed RA. Simulation analysis for detection of partial discharge inside oil insulator of high voltage transformer. Des Eng. 2021;51:1178–86.
[4] Mohammed RA, Hamoodi SA, Hamoodi AN. Comparison between two calculation methods for designing a stand-alone PV system according to Mosul city basemap. Open Eng. 2021;11:782–9.
[5] Gunawardana DMS, Kanchana AAT, Wijesingha PM. A matlab simulink model for a partial discharge measuring system. Department of Electrical Engineering, University of Moratuwa, Katubedda, Sri-Lanka, Electrical Engineering IEEE Conference; 2015. p. 29–34.
[6] Arief Y, Izzati W, Adzis Z. Modeling of partial discharge mechanisms in solid dielectric material. Int J Eng Innovative Technol. 2012;1:315–20.
[7] Fidan M, Ismailoglu H. A novel partial discharge calibrator design via dual microcontroller and high speed Dac Kocaeli University. 41040, Izmit, Kocaeli. TURKIYE: Faculty of Engineering. Department of Electrical Engineering High Voltage Laboratory; 2017.
[8] Gunnarsson O, Bergman A, Rydler KE. A method for calibration of partial discharge calibrators. IEEE Trans Instrum Meas. April 1999;48(2):453–6.
[9] Hamoodi SA, Hamoodi AN, Hameed FI. Pitch angle control of wind turbine using adaptive fuzzy-PID controller. EAI Endorsed Transactions on Energy Web; 2020.
[10] Mor AR, Castro LC, Muñoz FA. A magnetic loop antenna for partial discharge measurements on GIS. Delft Univ Technology, Electr Sustain Energy Department, Delft, Netherlands, Electr Power Energy Syst J homepage. 2020;115:105514.
[11] Wu J, Mor AR, Nes PV, Smit JJ. Measuring method for partial discharges in a high voltage cable system subjected to impulse and superimposed voltage under laboratory conditions. Netherlands, Electr Power Energy Syst J homepage. 2020;115:1–12.
[12] Pirker A, Schichler U. Partial discharge measurement at DC voltage – Evaluation and characterization by NoDi∗ pattern. IEEE Trans Dielectr Electr Insul. 2018;25(3):883–91.
[13] Baghelkar N, Dubey A. A review of study and analysis of partial discharge for different insulation materials with capacitance value. Int J Eng Technol Manag Res. 2020;7(12):64–6.
[14] Krbal M, Pelikan L, Stepanek J, Orsagova J, Kolcunova I. A physical calibrator for partial discharge meters. Dep Electr Power Engineering, Brno Univ Technology, Energies, MDPI. May 2019;12:1–10.
[15] Kai X, Genghua L, Yan J, Ziqi Ch, Jian L. "Development of partial discharging simulation test equipment," State Power Company Limited Training Center, Changchun, 1st International Global on Renewable Energy and Development (IGRED 2017). IOP Conf. Series; 2017. p. 1–9.
[16] Jing W, Yong W. Research and development of simulated training system for detection of partial discharge of high-voltage equipment. Acad J Guangdong Polytech Water Resour Electr Eng. 2015;13(1):34–7.
[17] Yue H, Chiampi M, Crotti G. Performance evaluation method and system development for partial discharge detector based on simulation of electric discharge schematic. J Electr Eng. 2015;10(5):87–93.
[18] Hamoodi SA, Al-Karakchi AA. Studying performance evaluation of hybrid E-bike using solar photovoltaic system. Bull Electr Eng Inform. 2022;11(1):59–67.
[19] Gupta AK, Ray S. Modeling of calibration circuit for partial discharge measurement. BTech Department of Electrical Engineering, National Institute of Technology. Rourkela: 2013.
[20] Merev A, Karaman I. implementation and analysis of a reference partial discharge measurement system, TUBITAK National Metrology Institute (UME), Gebze Yerles¸kesi, 41470 Gebze, Kocaeli, Turkey. MAPAN-Journal Metrology Soc India. 2019;34(1):43–8.
[21] Havunen J, Hallstrom J. Application of charge-sensitive preamplifier for the calibration of partial discharge calibrators below1 PC. Conference on precision electromagnetic measurements'. Paris, France: (CPEM); 2018. p. 8–13.
[22] Daulay MSH, Khayam U. Background noise level in high voltage laboratory measured by using partial discharge current sensors. International conference on high voltage engineering and power system (ICHVEPS). Bali, Indonesia: 2017. p. 2–5.
[23] Garnacho F, Alvarez F, Ramirez A, Ortego J, Sanchez-Uran MA. Reference PD generator for sensitivity checking of measuring instrumentation to be used for continuous on-line PD Monitoring. CIGRE Paris Session. Paris, France: 2018. p. 26–31.
[24] Hamoodi SA, Hamoodi AN, Hameed FI. armature control of a dc motor based on programmable logic controller. Przegląd Elektrotech. ISSN 0033-2097, R. 98 NR 5/202. 2022;2022(5):110–4.
[25] Hassan W, Hussain GhA, Mahmood F, Amin S. Effects of environmental factors on partial discharge activity and estimation of insulation lifetime in electrical machines. IEEE Access Multidisciplinary Rapid Review, Open Access J. 2020;8:108491–502.
[26] Hussain GA, Kumpulainen L, Kluss JV, Lehtonen M, Kay JA. The smart solution for the prediction of slowly developing electrical faults in MV switchgear using partial discharge measurements. IEEE Trans Power Del. 2013;28(4):2309–16.
[27] Pan C, Chen G, Tang J, Wu K. Numerical modeling of partial discharges in a solid dielectric-bounded cavity: a review. IEEE Trans Dielectr Electr Insul. 2019;26:981–1000.